small methods
www.small-methods.com

Near Quantitative Ligation Results in Resistance of DNA Origami Against Nuclease and Cell Lysate

*Kirankumar Krishnamurthy, Arivazhagan Rajendran, Eiji Nakata, and Takashi Morii**

There have been limited efforts to ligate the staple nicks in DNA origami which is crucial for their stability against thermal and mechanical treatments, and chemical and biological environments. Here, two near quantitative ligation methods are demonstrated for the native backbone linkage at the nicks in origami: i) a cosolvent dimethyl sulfoxide (DMSO)-assisted enzymatic ligation and ii) enzyme-free chemical ligation by CNBr. Both methods achieved over 90% ligation in 2D origami, only CNBr-method resulted in ≈80% ligation in 3D origami, while the enzyme-alone yielded 31–55% (2D) or 22–36% (3D) ligation. Only CNBr-method worked efficiently for 3D origami. The CNBr-mediated reaction is completed within 5 min, while DMSO-method took overnight. Ligation by these methods improved the structural stability up to 30 °C, stability during the electrophoresis and subsequent extraction, and against nuclease and cell lysate. These methods are straightforward, non-tedious, and superior in terms of cost, reaction time, and efficiency.

1. Introduction

In recent years, DNA origami has emerged as a novel technique for constructing nano[1] to micrometer scale materials[2] with sub-nanometer addressability and is utilized for various materials,[3] chemical,[4] and biological applications.[5] Despite the proof-of-concept demonstrations, the broad applicability of DNA origami is hampered by their stability issues. When subjected to thermal treatments, the origami structures melt around 50–60 °C.[6] While it has been reported that certain structures exhibit a slightly improved stability of 65–70 °C when evaluated using fluorescence spectroscopy and SYBR Green as an intercalator with Mg^{2+} concentrations in the range of 10–100 mM, it is important to treat these results with caution and to consider the limitations and potential inaccuracies associated with this method.[7] The origami cuboid failed to withstand the mild mechanical force applied during the structural analysis by atomic force microscopy (AFM).[8] These structures are stable between the pH of 4.5–10 while denaturing at a lower pH.[9] The samples may also be stored in pure water for several applications. However, the triangular origami exhibited several defective sites in pure water.[10] The origami undergo digestion against nucleases such as DNase I (the most abundant nuclease in blood and plasma) either in vitro[11] or in cell culture medium,[12] and T7 endonuclease I.[11]

The buffers for most origami synthesis contain 5–20 mM Mg^{2+} as they cannot be folded without Mg^{2+}.[9a] However, when the folded origami was exchanged into an Mg^{2+}-free buffer, its structural integrity changed depending on its super/globular structure and buffer composition. For example, when exchanged into Tris, Tris-acetic acid-EDTA (TAE), and phosphate buffers, the 6-helix bundle retained the folded structure, while the 24-helix bundle remained intact only in Tris buffer.[10] Similar results were also observed for a tubular origami, which upon exchanged into the crystallization buffers of various proteins, HEPES, PEPES, and 2-(N-morpholino)ethanesulfonic acid (MES).[9a] The phosphate buffers and EDTA present in TAE could competitively replace the origami-bound Mg^{2+}, thereby destabilizing the structure. The structure-dependent denaturation of the origami in low magnesium tissue culture medium was also reported.[12] Regarding other cations, the origami is unstable in the presence of K^+, Ca^{2+}, and NH_4^+, which are usual supplements in protein crystallization buffers.[9a] Overall, these findings indicate that Mg^{2+} is necessary to ensure the folded structure, while ionic strengths in physiological conditions are however much lower than needed to ensure the origami stability. The typical Mg^{2+}, Na^+, and K^+ concentrations in cell culture media are 0.04–0.8, 150, and 5.5 mM, respectively.[13] Although some origami maintain a stable structure under these conditions, mainly depending on the super/globular structure and crossover spacing, this environment is unsuitable for most origami materials.[14] Not only biological, but also material applications such as spray coating require low magnesium.[15]

Several methods have been attempted to address the stability issues of origami.[13,16] The photo-cross-linking by 8-methoxypsoralen,[6] and the formation of cyclobutane pyrimidine dimers[17] introduce the covalent linkages for this purpose.

K. Krishnamurthy, A. Rajendran, E. Nakata, T. Morii
Institute of Advanced Energy
Kyoto University
Gokasho, Uji, Kyoto 611-0011, Japan
E-mail: t-morii@iae.kyoto-u.ac.jp

The ORCID identification number(s) for the author(s) of this article can be found under https://doi.org/10.1002/smtd.202300999

DOI: 10.1002/smtd.202300999

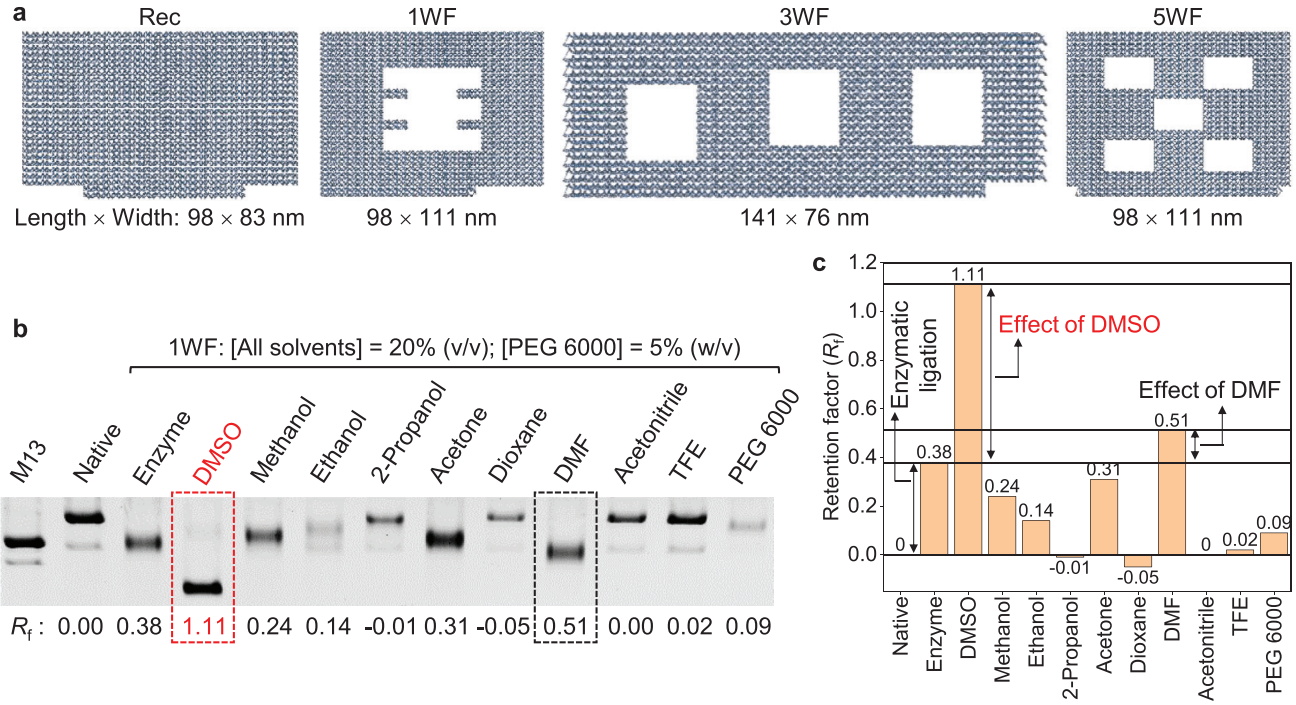

Figure 1. a) Graphical outline of the Rec, 1WF, 3WF, and 5WF. b) Native AGE of the non-ligated (Native) and ligated 1WF in the absence (lane marked Enzyme) and presence of various cosolvents/cosolute. The estimated R_f is given below the gel. [1WF] = 15 nM (in reaction mixture) and 3 nM (for AGE); [Cosolvents] = 20% (v/v); [PEG 6000] = 5% (w/v); [Ligase] = 2400 U; [Reaction buffer] = 1× PNK buffer, pH 7.5; [ATP] = 0.5 mM; reaction temperature = 37 °C; and reaction time = overnight. c) Plot of the various cosolvents/cosolute and the estimated R_f from AGE in (b).

Other methods include the coating with the lipid bilayer,[18] virus capsid[19] and other proteins,[20] cationic polymers,[21] and spermidine.[22] Besides these non-natural treatments, we have demonstrated the optimum conditions for enzymatic ligation of staple nicks in 2D origami.[23] However, this method resulted in only 31–55% ligation efficiency and the thermal stability improved by only 5–20 °C, depending on the structure. The only other ligation method reported on the full-size origami is the chemical ligation by *N*-(3-dimethylaminopropyl)-*N*′-ethylcarbodiimide (EDC).[24] Despite the interesting demonstration, it requires tedious processes, batch modification of the 3′-end of all the ≈226 staples is necessary, requires the amino-modified ddNTPs and terminal deoxynucleotidyl transferase in addition to T4 polynucleotide kinase (PNK), and releases isourea as a by-product. Moreover, this method creates an unnatural backbone linkage with an amino group at each ligation site that can be easily cleaved upon treatment with mild acids.

Here, we report two near quantitative ligation methods for the native phosphate backbone linkage at staple nicks in full-size 2D and 3D origami. The first method relies on the ligation by T4 DNA ligase, while the presence of a cosolvent dimethyl sulfoxide (DMSO) drives the ligation reaction from halfway to near completion. The second method is the enzyme-free chemical ligation[25] by cyanogen bromide, a method previously demonstrated for duplex DNA (dsDNA) ligation.[26] To demonstrate the application of these methods, we have tested the stability of the ligated origami against thermal treatments, during the electrophoresis and subsequent extraction, nuclease digestion, and cell lysate.

2. Results

2.1. Screening of Cosolvents

The previous investigations of the effect of DMSO on the ligation indicated that it either increased the extent of ligation reaction,[27] or showed no effect,[28] or increased the specificity while decreasing the efficiency.[29] This motivated us to test the effect of DMSO and other solvents on the ligation of DNA origami. The initial ligation experiments were carried out with four different 2D DNA origami structures, namely rectangle (Rec),[1] and frame-shaped origami containing 1 (1WF),[30] 3 (3WF)[31] and 5 wells (5WF)[32] (**Figure 1**a; Table S1, Supporting Information). Several organic solvents were screened to determine the best-performing cosolvent on the enzymatic ligation of origami using 1WF (see Experimental Section). All the staple stands were purified to remove kinase inhibitors such as ammonium and phosphate ions, 5′-phosphorylated with ≈100% yield by following our previous report,[23] and utilized to fold M13mp18. After folding, the excess staples were removed by spin column filtration, and the origami was ligated by T4 DNA ligase in the absence or presence of cosolvent. The following conditions optimized in our previous study[23] for the ligation of staple nicks in 2D origami were used for the initial cosolvent screening: 10–30 nM of origami, 0.5 mM of adenosine triphosphate (ATP), 2400 U of ligase, overnight reaction at 37 °C, in 1× PNK buffer, pH 7.5. The amount of cosolvents and cosolute polyethylene glycol 6000 (PEG 6000) used were 20% (v/v) and 5% (w/v), respectively.

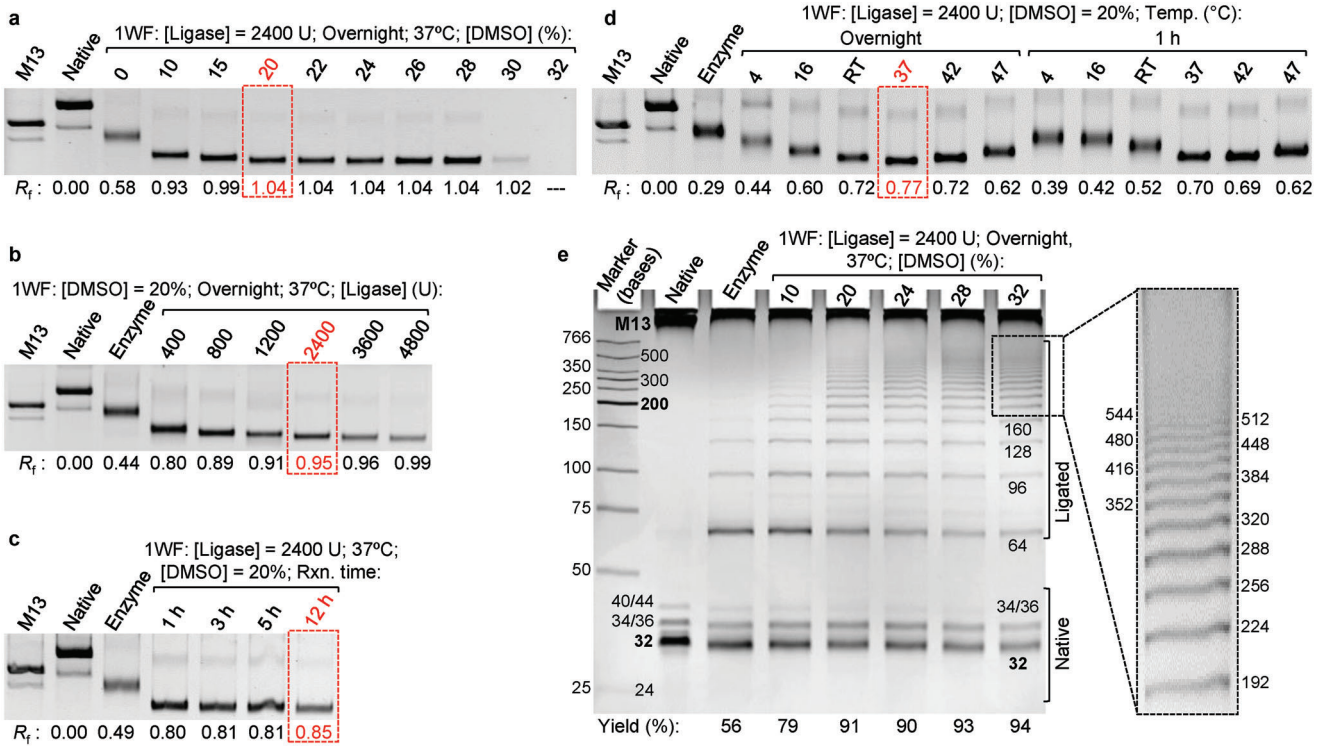

Figure 2. Native AGE for the identification of a) optimum DMSO concentration, b) amount of ligase required, c) reaction time, and d) reaction temperature of the enzymatic ligation of 1WF. e) Denaturing PAGE of the non-ligated (Native) and ligated 1WF in the absence (Enzyme) and presence of various amounts of DMSO. The exact length of the marker strands and approximate length of the ligated strands are mentioned. Conditions listed in the Figure 1 caption were used, except for the variables mentioned in each case. The image on the right is a magnified and contrast-adjusted section of the original gel on the left. In addition, the following concentrations are applicable: [1WF] = 15 nM (in reaction mixture and for PAGE) and 3 nM (AGE).

The agarose gel electrophoresis (AGE) image in Figure 1b depicts the relative migration of the non-ligated (native) and the origami ligated in the absence and presence of cosolvents/cosolute. The ligation of the staples influences the globular structure of the origami and leads to a relatively faster migration in the AGE compared to the native origami, which serves as a marker for the extent of the ligation reaction.[23] Therefore, the faster the migration in the AGE, the better the ligation of the staple nicks. The 1WF ligated in the presence of DMSO showed the fastest migration with the retention factor (R_f) of 1.11, while it is 0.38 for the enzymatically ligated origami without any cosolvent/cosolute (Figure 1b,c). Because DMSO alone did not influence the migration of native origami (Figure S1, Supporting Information), this result indicated that the appropriate cosolvent could enhance the enzymatic ligation of origami. Dimethyl formamide (DMF) showed mild improvement in the enzymatic ligation, while acetone exhibited almost no change. According to the R_f values, all other solvents and PEG 6000 inhibited the enzymatic ligation either partly or entirely. Based on these results, we have identified DMSO as the best-performing cosolvent.

2.2. Optimization of the Conditions

To fine-tune the conditions, the ligation was performed by varying the amount of DMSO (**Figure 2**a). The increase in migration of the ligated origami was observed upon increasing the amount of DMSO. The highest R_f value was obtained for the DMSO concentration of 20%, and increasing its amount any further didn't increase the R_f. At the DMSO concentration of 30–32%, the origami band started to disappear from the gel, possibly it was precipitated and removed from the solution during the spin column filtration carried out before the AGE analysis. Under this optimal solvent composition of 20% DMSO, the amount of ligase required is then evaluated. The fastest migration was observed for the ligase concentration of 1200–2400 U, and increasing the enzyme to 3600 or 4800 U resulted in only a subtle increase in the origami migration (Figure 2b). From these results, we have concluded that 2400 U of ligase is optimum for ligating a full-size DNA origami.

In all the above-experiments, the duration of the ligation reaction was overnight. To check the optimal duration, the reaction time was varied from 1 to 12 h. When compared to the cosolvent-free enzymatic reaction carried out overnight, the cosolvent-assisted reaction for 1 h exhibited a faster migration of origami (Figure 2c), but the reaction requires overnight to saturate. In addition, the 1 h reaction with 100 U of ligase in the presence of 20% DMSO (R_f of 0.61) roughly equals the enzyme-alone reaction carried out overnight with 2400 U of ligase (R_f of 0.59, Figure S2, Supporting Information). Next, the ligation was carried out at various temperatures for 1 h and overnight (Figure 2d). Irrespective of the reaction time, the temperature of 37 °C resulted in the best ligation. AGE analyses were carried out also for other origami, and the highest R_f was obtained for the samples ligated

in the presence of DMSO (Figure S3, Supporting Information). Taken together all the above observations, we conclude the following optimized conditions: 20% of DMSO, 2400 U of ligase, 0.5 mM of ATP, 1× PNK buffer, pH 7.5, and overnight reaction at 37 °C. These optimized conditions were used from this point onwards, except for the variables mentioned in specific cases.

2.3. Estimation of Ligation Yield

To visualize the ligated staples and to estimate the ligation efficiency, denaturing polyacrylamide gel electrophoresis (PAGE) was carried out. In the denaturing PAGE (Figure 2e; Figure S4a, Supporting Information), the native 1WF exhibited an intense band corresponding to the length of 32 bases and three minor bands with 24, 34/36, and 40/44 bases that correlate well with the original staple design (Table S1, Supporting Information). The intense band in the well is due to the M13 scaffold. The cosolvent-free ligation resulted in a relatively smaller number of ligated bands with low intensity. The addition of 10% DMSO increased the number of ligated bands and their intensity. Increasing the amount of DMSO further increased the length distribution and intensity of the bands. The PAGE analysis further indicated that 20% DMSO is sufficient for the ligation. The 16-point ligations with the ligated staple distribution from ≈64 to ≈544 bases were characterized. This staple distribution corroborates with the original design of 1WF, as theoretical ligation of a minimum of 2 and a maximum of 32 staples could be possible. Interestingly, the ligation reaction was not inhibited at a higher DMSO concentration of 32%, indicating that the problem in the AGE could be due to the loss of origami during the spin column filtration. A small amount of staples with 32 and 34/36 bases were present in all the ligated samples, characterized as excess unpurified staples (Figure S4b, Supporting Information). These excess staples were quantified, and the ligation yields were corrected accordingly. The estimated ligation efficiencies were 91 and 94% for the DMSO concentration of 20 and 32%, respectively.

The other reaction conditions, such as the optimum amount of ligase required, reaction time, and temperature, were also verified by the denaturing PAGE analyses (Figures S5–S7, Supporting Information), and similar results to that of the AGE analyses were obtained. To check the effect of cosolvent and the suitability of the optimized conditions in a broader context, the ligation reactions were carried out also on Rec, 3WF, and 5WF (Figure S8, Supporting Information). Comparable results were obtained for all the tested structures, indicating that the effect of cosolvent is universal and independent of the super/globular structure, at least for the 2D origami.

2.4. Chemical Ligation of 2D Origami

Next, we performed the chemical ligation by CNBr on the 2D origami structures. The procedures are the same until the origami folding as in the case of cosolvent-assisted enzymatic ligation. Afterwards, the samples were purified, exchanged into MES buffer, and ligated on the ice. The gel mobility shift assay indicated the success of the chemical ligation (**Figure 3**a). Though the ligation reaction proceeded with as low as 0.05 M, it required 0.5 M of CNBr for the completion of the reaction. Further, we analyzed the role of the relative ratio of MES and CNBr. The data in Figure 3a,b indicated that the ratio of 1:2 of CNBr:MES with the absolute concentration of 0.5 M of CNBr is required for the reaction to saturate. In the absence of phosphorylation, the addition of CNBr to the 1WF did not cause any observable change in the AGE migration compared to the native 1WF in the absence of CNBr (Figure 3c). The R_f of 0.55 was the same for the reaction time of 5 to 15 min, indicating that the reaction was completed within 5 min and extending the reaction time further did not influence the ligation (Figure 3c). Also, chemical ligation performs better than cosolvent-free enzymatic ligation (R_f is 0.38).

In addition to the fast-migrating band, a distinct slow-migrating band with an average yield of 18% was observed for the CNBr- ligated samples, with the migration very similar to the native origami. Such a slow-migrating faint band was also observed for the native and enzymatically ligated samples in the absence and presence of DMSO with average yields of 3, 6, and 11%, respectively (Figure 2a–d). The fast-migrating band corresponds to the monomer 1WF, while the slow-migrating band is due to dimer formation along the helical axis of the duplexes in origami, based on the analyses by AGE (Figure S9, Supporting Information) and AFM (Figure 3d; Figure S10, Supporting Information). The dimer band in AGE was stable until the melting point of origami (Figure S11a, Supporting Information). Also, we could successfully isolate the dimer fraction and record AFM images (Figure 3d). These observations suggest the non-specific inter-origami covalent bond formation during the ligation, though additional research is needed to prove this.

A similar trend in AGE was observed for all other tested origami (Figure S11b, Supporting Information). By systematically investigating the effects of buffer types and initial and final pH of the reaction mixtures on the ligation of 1WF (Note S1, Figures S12,S13, and Table S2, Supporting Information), we concluded the following optimized conditions for the CNBr-mediated ligation: 15 nM of origami in 1 M of MES buffer, pH 7.6, 5 mM of Mg^{2+}, 0.5 M of CNBr, and 5 min reaction on ice. These optimized conditions were used for further experiments except for the variables mentioned in specific cases.

Denaturing PAGE analysis indicated that the number and the intensity of CNBr-ligated bands were higher than that of the cosolvent-free enzymatically ligated sample (Figure 3e). The estimated ligation efficiencies for 1WF were 93 and 58% for the former and latter methods, respectively. The CNBr-mediated ligation was also successful for other origami, and the estimated ligation efficiencies were 91, 85, and 82% for Rec, 3WF, and 5WF, respectively (Figure S14, Supporting Information). The PAGE analyses of all three ligation methods indicated that DMSO and CNBr methods yield nearly identical ligation efficiencies (Figure S15, Supporting Information).

2.5. Ligation of 3D Origami

After successfully demonstrating ligation for 2D origami, the methods were applied to four different 3D origami structures, such as hexagonal prism in the open (HPO) and closed (HPC) forms,[33] sphere (SPH),[18] and 12 helix bundle ring (Ring),[34] (**Figure 4**a; Table S3, Supporting Information). PAGE analyses

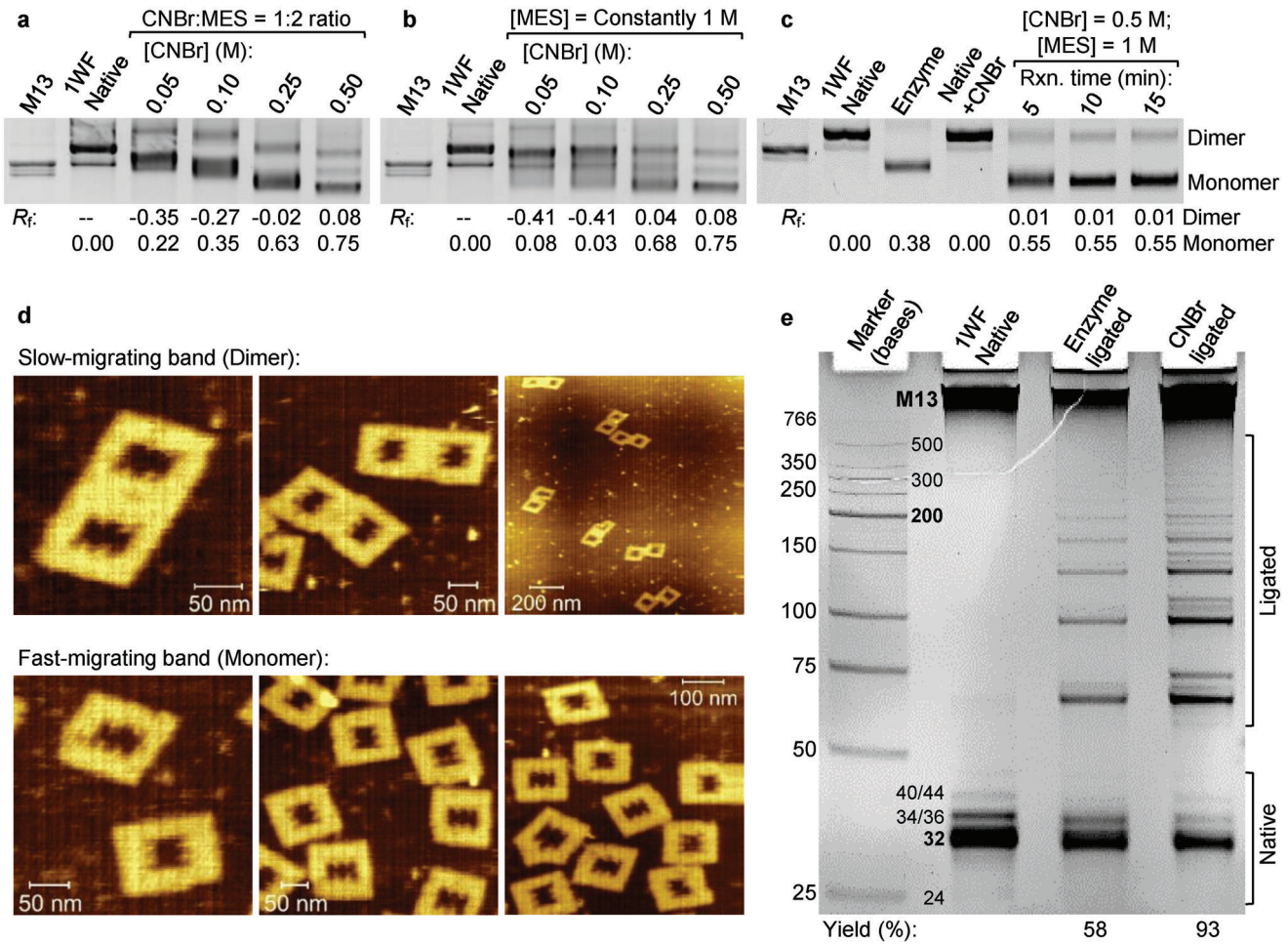

Figure 3. Native AGE of the chemically ligated 1WF by varying the a,b) amounts of CNBr and MES and c) reaction time. d) Representative AFM images of the monomer and dimer bands of 1WF extracted from AGE. These images correspond to the condition of 5 min ligation, as shown in (c). e) Denaturing PAGE analysis of native, enzymatically ligated, and CNBr-ligated 1WF. Except for the variables mentioned in each case, the conditions are the same as in the Figure 1 caption. In addition, the following conditions are applicable: [CNBr] = 0.5 M; [MES] = 1 M, pH 7.6; [DMSO] = not used; reaction temperature = 37 °C (enzymatic ligation) and 4 °C (CNBr ligation); and reaction time = overnight (enzymatic ligation) and 5–15 min (CNBr ligation).

indicated the superior ligation by CNBr over DMSO-assisted enzymatic ligation for HPO (Figure 4b; Figure S16a, Supporting Information). A similar pattern was observed in the ligation of other 3D origami as well (Figure S16b, Supporting Information). The estimated ligation efficiencies were 79, 76, 72, and 73% for HPO, HPC, SPH, and Ring, respectively. These results indicated that only CNBr works effectively to ligate 3D origami. Based on our observations, the optimized reaction conditions are listed in Figure 4c.

2.6. Analysis of Thermal Stability

Next, to achieve our objective of stable origami under various conditions, we tested the stability against thermal treatment, purification by AGE, DNase I, and cell lysate as representative conditions for the materials and biological applications. At first, the resistance of the native and ligated 1WF to thermal treatment was investigated by UV-melting analysis (**Figure 5**a, left). Due to the presence of multiple strands with different sequences and lengths, the melting patterns of both native and ligated 1WF did not fit into the two-state (duplex and single-stranded) transition. The estimated predominant melting points (T_m) of native 1WF, ligated by enzyme alone, and in the presence of DMSO were ≈63, ≈65, and ≈73 °C, respectively. This indicated that DMSO-method significantly enhances the thermal stability of 1WF with an estimated ΔT_m of 10 °C. In addition, a notable hypochromicity was also observed for the ligated samples, with the highest value observed in the presence of DMSO (20% hypochromicity at 80 °C). The melting analyses performed for other origami also indicated similar results (Figure S17 and Table S4, Supporting Information).

The melting analysis was then carried out for the CNBr-ligated samples (Figure 5a, middle). The mere presence of CNBr in the native 1WF had a negligible effect. As in the case of DMSO-method, chemical ligation also increased the T_m and the estimated ΔT_m was 8 °C. The reaction time of 5–15 min had a subtle effect on the melting profile of 1WF. Further, a relatively steeper

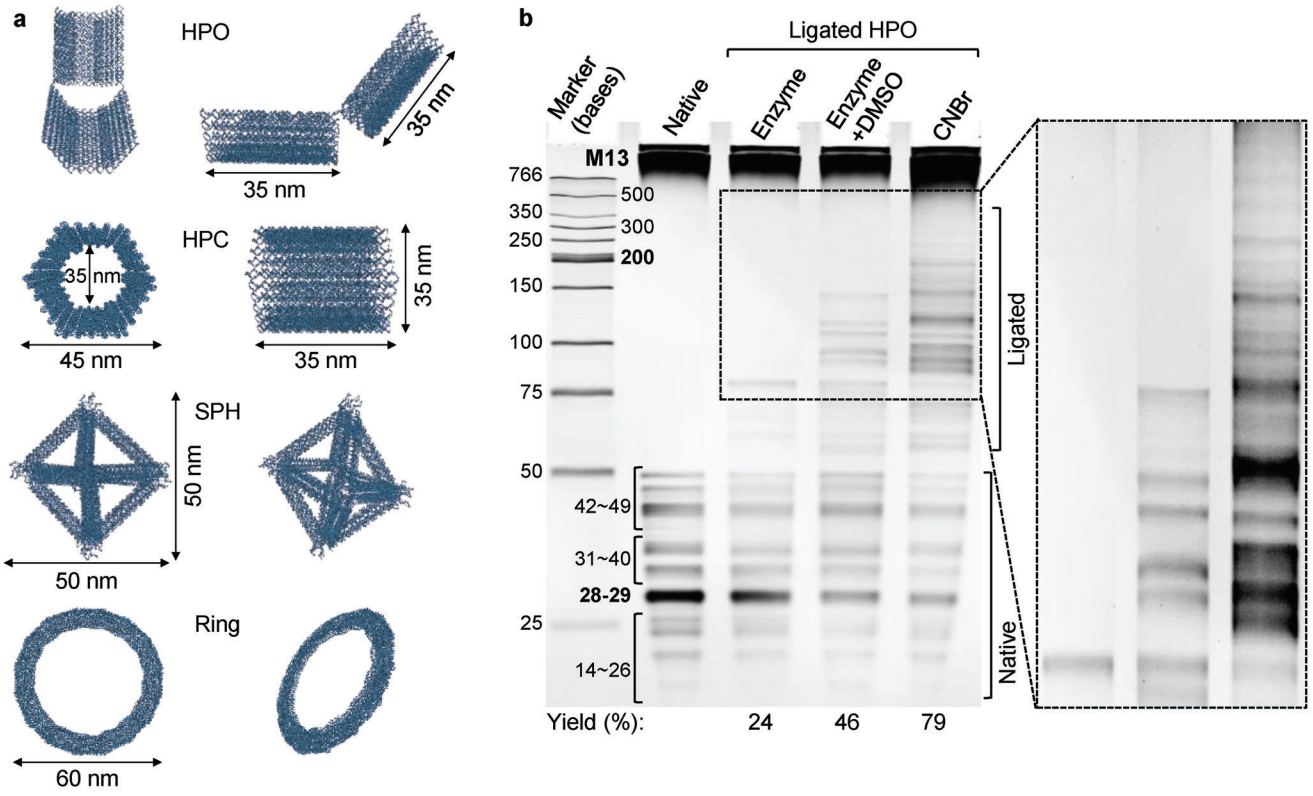

c

Reagents	PNK reaction	Ligation reactions		
		Enzyme	Enzyme+DMSO	CNBr
Staple mixture	40-280 nM (9-63 μM of 5′-termini)	--	--	--
Origami	--	15 nM (3.4 μM of 5′-P)	15 nM (3.4 μM of 5′-P)	15 nM (3.4 μM of 5′-P)
PNK	20 U	--	--	--
Ligase	--	2400 U	2400 U	--
Buffer	1× PNK (pH 7.5)	1× PNK (pH 7.5)	1× PNK (pH 7.5)	1 M MES (pH 7.6)
ATP	1 staple:2 ATP	0.5 mM	0.5 mM	--
DMSO	--	--	20% (v/v)	--
CNBr	--	--	--	0.5 M in CH_3CN
Rxn. time	30 min	overnight	overnight	5 min
Rxn. temp.	37°C	37°C	37°C	4°C
Efficiency	~100%	2D: <55%, 3D: <36%	2D: >90%, 3D: <50%	2D: >90%, 3D: ~80%

Figure 4. a) Schematic illustrations of the 3D origami used in this study. b) Denaturing PAGE of native and ligated HPO. The image on the right is a magnified and contrast-adjusted section of the original gel on the left. Optimized conditions listed in (c) were used. c) List of optimized conditions for the PNK reaction, enzymatic ligations with and without DMSO, and CNBr-mediated chemical ligation. These conditions are valid for both 2D and 3D origami.

curve observed for the ligated samples indicates that the melting profile approaches closer to a two-state model due to the reduction of the unligated 32 bp portion melting at ≈55 °C. A similar trend in melting profile was also observed for all other 2D origami (Figure S18 and Table S5, Supporting Information). The native HPO melted at 57 °C (Figure 5a, right). The enzymatic ligation of HPO in the absence and presence of DMSO led to a ΔT_m of 2 °C, and the observed hypochromicities were 9 and 30%, respectively. The CNBr-ligated sample exhibited a ΔT_m of 10 °C without hypochromicity. Similar melting patterns were also observed for other 3D origami (Figure S19a and Table S6, Supporting Information).

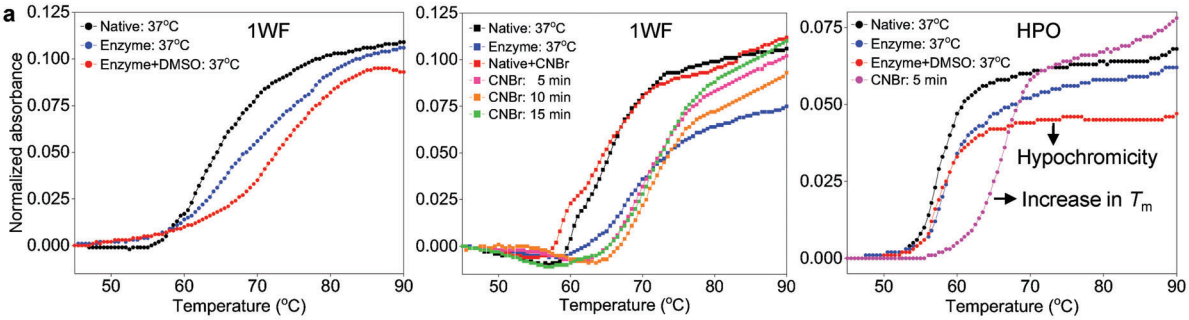

Method: UV-visible	1WF Native	Enz.	Enz. +DMSO	1WF Native	Native +CNBr	Enz.	CNBr, Time (min) 5	10	15	HPO Native	Enz.	Enz. +DMSO	CNBr (5 min)
T_m (°C)	63	65	73	63	63	67	71	71	71	57	59	59	67
% Hypo. @ 80°C	--	10	20	--	--	35	16	27	11	--	9	30	--

Method: AFM	Native	Enz	Enz.+DMSO	CNBr (5 min)		Native	CNBr (5 min)
1WF: T_m (°C)	50	60	65	70	HPO	50	65

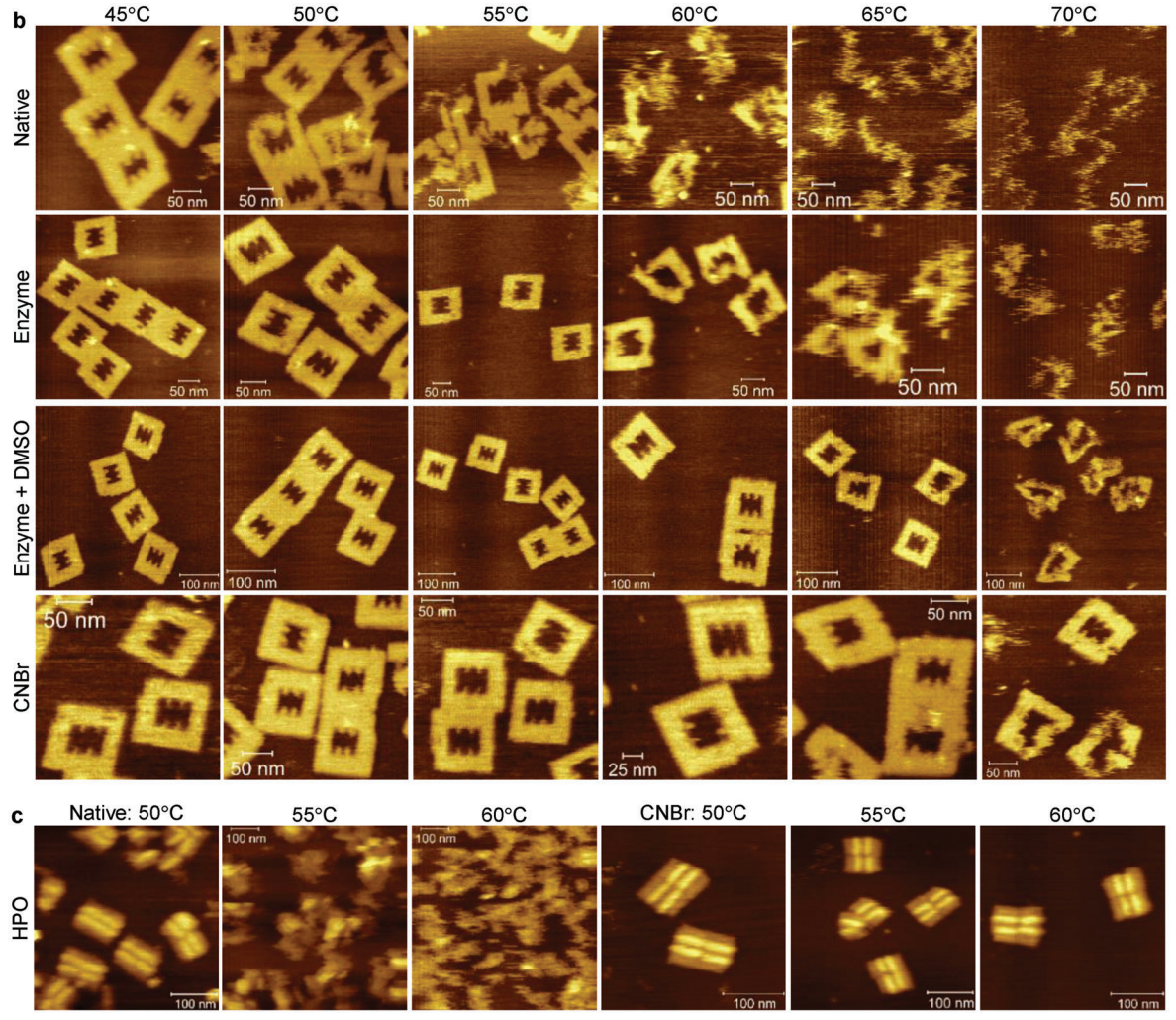

Figure 5. a) UV-melting analyses of native, enzymatically ligated 1WF in the presence of DMSO (left), chemically ligated 1WF (middle), and HPO (right). Table at the bottom lists the T_m and % hypochromicity. Representative AFM images of the native and ligated b) 1WF and c) HPO imaged after treating at the indicated temperatures. Optimized conditions listed in Figure 4c were used.

The structural resistance against thermal treatment was then investigated by AFM (Figure 5b). Note that we have assessed the stability of the entire DNA origami shape by AFM and not the melting temperature (T_m). The native 1WF was stable at 45 °C, notable damages were seen at 50 °C, and the topology was completely damaged at 55 °C. The enzymatically ligated origami was stable at 55 °C, visible damages were seen at 60 °C, and the origami was completely denatured at 65 °C. Interestingly, when ligated by DMSO and CNBr methods, the 1WF was stable at 65 and 70 °C, respectively. Similar results were obtained for other origami, and the observed increases in structural stability against thermal treatment were 15, 15, and 30 °C for Rec, 3WF, and 5WF, respectively, with both the ligation methods (Figures S20–S23, Supporting Information). Collectively, these methods improved the structural stability against heat treatment of the 2D origami from as low as 15 °C to as high as 30 °C, depending on the structure. As for the 3D structures, the native HPO was stable until 45 °C, slight damages were seen at 50 °C, while completely disintegrated at 55 °C (Figure 5c; Figure S24, Supporting Information). The CNBr-ligated sample was stable until 60 °C and disintegrated at 65 °C. A similar stability pattern was also observed for the Ring structure (Figure S25, Supporting Information). Overall, these observations indicated that the ligation improves the structural stability against heat treatment of both 2D and 3D origami.

2.7. Stability During Electrophoresis and Subsequent Extraction

Next, the samples were electrophoresed by AGE, excised the target bands, extracted the origami, and analyzed by AFM. Native 1WF failed to retain the stable topology (Figure S26, Supporting Information). In contrast, the 1WF ligated under DMSO condition and CNBr-ligated monomer and dimer forms fully retained the stable structure. We then checked the electrophoretic stability of HPO as a representative example of 3D origami. There were two distinct bands in AGE when native HPO was electrophoresed (Figure S19b, Supporting Information), and the samples in both bands were completely disintegrated (Figure S27, Supporting Information). The presence of NaCl failed to stabilize the native HPO. Notable improvements were seen for the HPO ligated by CNBr, while it couldn't guarantee the completely folded topology. All the AGE analyses discussed above were performed without Mg^{2+} in the gel and running buffer. The presence of Mg^{2+} resulted in a stable structure for both native and CNBr-ligated HPO. These results collectively indicated that ligation overcomes the electrophoretic stability issues of 2D origami under Mg^{2+}-free conditions, while it fails for 3D origami.

2.8. Stability Against Nuclease

The stability analysis against nuclease indicated that the native Rec started to digest with 0.01 U of DNase I and almost completely digested with 0.1 U when incubated at 37°C for 1 h (**Figure 6**a, top). Notable digestion was observed for the cosolvent-free enzymatically ligated sample for the nuclease concentrations of 0.05–0.1 U. The samples ligated by DMSO and CNBr methods were completely stable for all the tested nuclease concentrations, except a tiny fraction was digested with 0.1 U of DNase I. AFM analysis indicated the similar trends with the estimated digestion yields of 100, 49, 13 and 7% for the native, enzyme, DMSO, and CNBr methods, respectively, for the nuclease concentration of 0.05 U (Figure 6a bottom, and S28). The native and enzymatically ligated HPO were significantly scissioned with 0.05–0.1 U of nuclease. DMSO and CNBr methods improved the stability until 0.05 U of nuclease, while a minor scission fragment was observed with 0.1 U of DNase I. It should be noted that the nuclease-digested fragments of Rec appeared as smearing bands, while only a single distinct digested band appeared for HPO along with the unscissioned fragment. This pattern was characterized by AFM, which indicated that rather than the digestion, the strands at the hinge region that connects the top and bottom parts of the HPO are scissioned, leading to the top and bottom fragments that might be migrating as a single band in AGE (graphics in Figure 6b). Being the 3D structure and having the non-planar duplex arrangement (square lattice 2D Rec consists of planar duplexes, while it is non-planar/zigzag in honeycomb HPO 3D structure), HPO exhibits better stability against nuclease than the 2D structures. The yields of scission were 93, 79, 51, and 16% for the native HPO, enzyme, DMSO, and CNBr methods with 0.05 U of nuclease (Figure 6b bottom, and Figure S29, Supporting Information). It is worth noting that a previous study reported a contradictory result regarding the susceptibility of a honeycomb structure to DNase I compared to two out of the three square lattice structures investigated.[35] Interestingly, the honeycomb structure showed a susceptibility in terms of reaction time that was comparable to the square lattice triangle structure. These results suggest that factors such as local flexibility or accessibility to the nuclease may play a more significant role in digestion/stability than the super/globular structure itself or the type of lattice.

Stability analysis was also performed using exonuclease. Due to its lack of specificity for the nick sites, lambda exonuclease was unable to digest the Rec, regardless of whether ligation was performed or not (Figure S30, Supporting Information). Previous reports also suggested that the exonucleases such as T7 exonuclease, Escherichia coli exonuclease I, lambda exonuclease, and bacterial exonuclease Exo I were unable to digest native origami structures.[14]

2.9. Stability Against Cell Lysate

The origami samples were then treated with the lysate of human embryonic kidney 293 (HEK293) cells for 12 h at room temperature (RT). The native Rec was unstable for any tested concentration of 10 000 to 40 000 cells (Figure 6c, top). The enzymatic ligation, DMSO, and CNBr methods resulted in stable origami for all lysate concentrations, except the band intensity slightly decreased with 40 000 cells. Similar results were also obtained by AFM (Figure 6c bottom; Figure S31, Supporting Information), and the estimated digested yields were 88, 43, 9, and 4% for native Rec, enzyme, DMSO, and CNBr methods with 10 000 cells in the lysate. The lysate-treated HPO samples were precipitated in the AGE wells, possibly due to the presence of Mg^{2+} in the gel and running buffer. However, AFM analysis indicated a similar pattern to the nuclease-treated samples (Figure 6d bottom; Figure

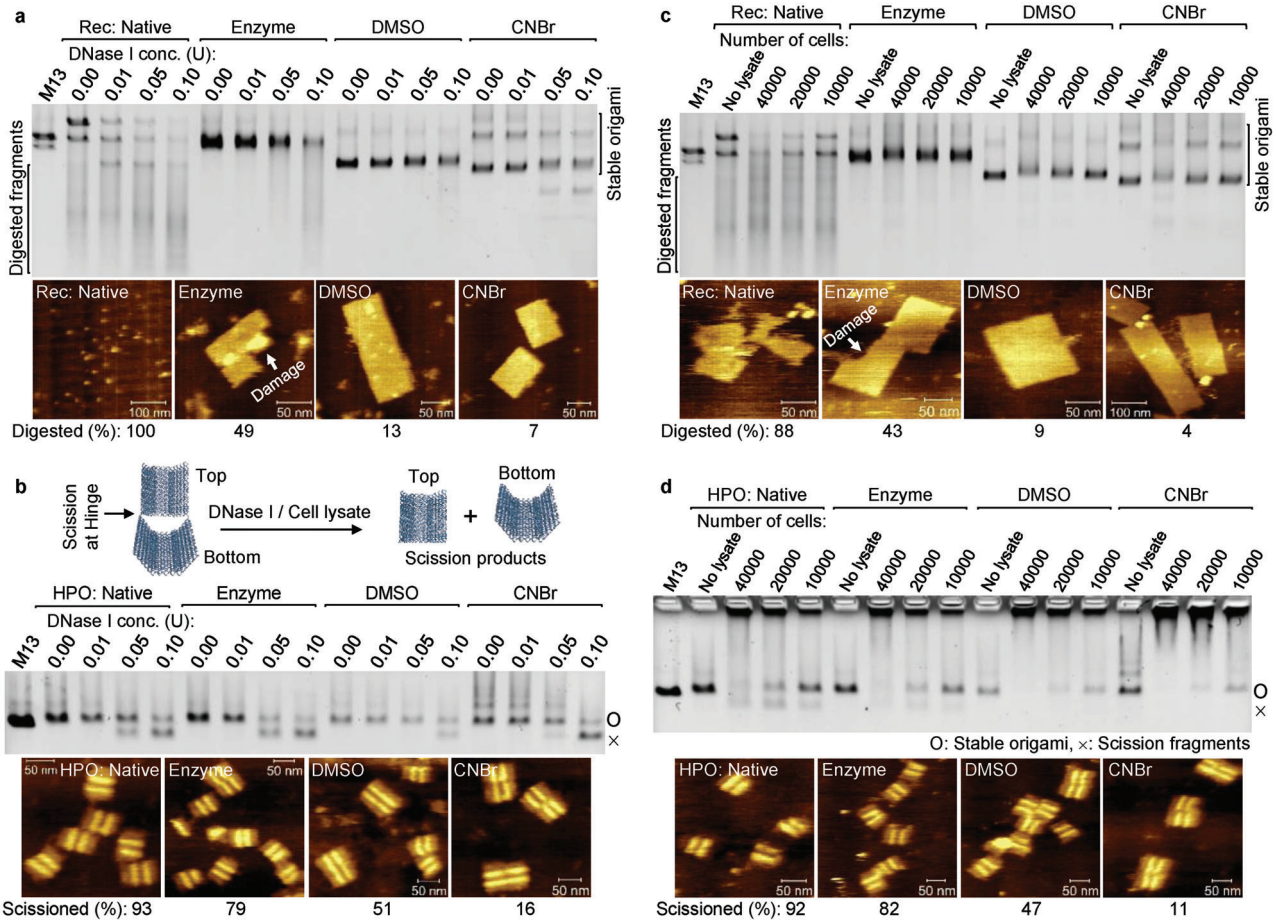

Figure 6. AGE of the a,b) DNase I and c,d) cell lysate treated a,c) Rec and b,d) HPO. For comparison, native and ligated samples by all three methods are included. Under each AGE image, representative AFM images of the origami treated with DNase I or cell lysate are also included along with the estimated digestion/scission yields. Optimized conditions listed in Figure 4c were used. [Rec/HPO] = 5 nM (in reaction mixture), [DNase I] = 0-0.1 U (AGE) and 0.05 U (AFM), [cell lysate] = 10 000-40 000 (AGE) and 10 000 cells (AFM); reaction temperature = 37 °C (DNase I) and RT (cell lysate), and reaction time = 1 h (DNase I) and 12 h (cell lysate).

S32, Supporting Information). As in the case of nuclease, lysate scissions the HPO at the hinge region and the estimated scission yields were 92, 82, 47, and 11%, respectively for the native, enzyme, DMSO, and CNBr methods for the lysate concentration of 10 000 cells. Overall, the above results indicated that ligation provides stability to both 2D and 3D origami against nuclease and cell lysate, which is important for biological applications. Ligation reduces the inter-duplex distance and leads to a rigid and tightly packed structure, which is anticipated as the cause of stability against nuclease/cell lysate because such a tightly packed structure possibly restricts the accessibility to the nuclease.

3. Discussion

3.1. Effect of DMSO on the DNA Duplexes in Origami

The effect of organic solvents on the stability, conformational change, and function of various nucleic acids, DNAzymes, ribozymes,[36] and several other enzymes has been investigated.[27,28,37] The organic cosolvents, including DMSO, enhanced the RNA ligation by the deoxyribozymes that require herbicides for their activity.[38] DMSO (10%, v/v) is shown to increase the extent of ligation reaction 2–3 fold for the 3′-labeling of RNA with T4 RNA ligase.[27] The presence of 10–30% DMSO enhanced the ligation of strands that contained mismatches at the ligation junction, while the reaction didn't occur any faster for the fully base-paired nicks.[28] In contrast, DMSO increased the specificity while decreasing the efficiency when the ligase detection reaction was carried out using Taq DNA ligase.[29] Despite these observations, the mechanism of the enhancement in the catalytic activity of ligases by DMSO is not clearly known. Most studies on the dsDNAs indicated that the thermal stability of base pairing decreases in a cosolvent mixture.[36] Such a destabilizing effect under a reduced water content was considered relevant to the catalytic function of DNA unwinding enzymes such as helicases.[39] For this reason, DMSO is often used to prevent the reassociation of template strands and was shown to enhance the polymerase chain reaction[40] and DNA sequencing.[41] Further, the rate of strand replacement in a 30 bp dsDNA was enhanced by adding DMSO.[42] Previous crystal structural analysis indicated that the DNA-ligase contacts around a nick site occupy a surface area of 2503 Å^2,[43] while

the available space around a nick site in origami was roughly estimated to be 2720 Å^2.[23] Therefore, the nick site in origami may provide a tight but mere sufficient space to accommodate the ligase while relaxing the duplexes would significantly benefit the ligase to effectively interact and seal the nicks. Thus, the duplex relaxation by the cosolvent mixture becomes crucial in the enzymatic ligation of origami.

Among the various factors, the osmotic pressure effect arising from the reduced water activity (a_w) and the relative dielectric constant (ϵ_r) effect that determines the efficiency of cation binding to the phosphate backbone were reasoned for the observed stability of dsDNAs in cosolvent mixture.[36] When compared to water, the estimated decrease in a_w for 20 wt.% DMSO and DMF were ≈0.05 and ≈0.02, indicating that the reduced water activity may not be playing a major role in the origami ligation. The ϵ_r of cosolvent-free water, DMSO, and DMF were 82, 72, and 70, respectively, indicating that the substantial decrease in ϵ_r might be relaxing the duplexes and subsequently enhancing the ligation efficiency (see Note S2 for additional discussion).[36]

3.2. Influence of DMSO on Ligase

As for the effect on the enzyme, the presence of DMSO as a cosolvent often enhances the stability of enzymes. For example, the half-life (in days) of chymotrypsin in pure water and in the presence of 20% (v/v) cosolvents followed the order: *tert*-butanol (2.5) < 2-propanol (7) < ethanol (9) < dioxane (13) < water (14) < methanol (16) < DMSO (more than 200 days).[37b] Since the overnight reaction was carried out at a relatively high temperature of 37 °C, the enhanced stability of the ligase would be beneficial. The DMSO-assisted ligation carried out at 37 and 47 °C had only a slight decrease in R_f (0.77 and 0.62, respectively) and so the ligation efficiency, while the ligation in the absence of DMSO exhibited a higher difference (0.51 and 0.10, respectively, Figure S33, Supporting Information). This may be interpreted as DMSO enhancing the stability of ligase even at elevated temperatures, and so the ligation efficiency. Another possibility is that the enzyme follows different kinetics in pure water and DMSO solution. Apart from the enzyme stability, DMSO and other organic solvents have been shown to induce the conformational change at the catalytic core of the enzymes (ex: lysozyme),[37a] which might be possible in ligase as well. Besides, if we consider the ligation efficiency of 2D and 3D origami, the effect of cosolvent on the enzyme is the same in both cases, while the duplex arrangement is different with multiple duplexes more tightly packed in 3D origami. The inability of DMSO to enhance enzymatic ligation on 3D origami indicates that the dominating factor could be the structural changes in DNA and not in the enzyme. A similar conclusion was also derived in a previous study using mismatches at the ligation junction that DMSO may not be acting directly on the enzyme while interacting with DNA and favorably orienting the ligation junction.[28]

3.3. Chemical Ligation

Regarding the chemical ligation, the tertiary amine [MES/N-methylmorpholine (NMM)] forms a quaternary ammonium base with CNBr, which activates the phosphomonoester group, followed by phosphodiester bond synthesis.[26a] In addition to forming a quaternary base, the tertiary amine should maintain the pH of the solution due to the rapid liberation of HBr during the reaction. MES buffer solves this problem and works better than NMM.[26a] When lower amounts of CNBr (0.05 to 0.1 M) were used, the ligation reaction proceeded only for the CNBr:MES ratio of 1:2. A higher amount of MES (i.e., 1 M) resulted in a smearing band with reduced R_f (Figure 3a vs. 3b), though a higher amount of MES is beneficial for maintaining the pH. This possibly indicates that the higher amount of MES affects the formation of the quaternary base and its role in activating the phosphomonoester group.

The reaction with alternative condensing agents such as imidazole derivatives[25] and EDC is either slow (several hours to a few days) or prone to give incomplete ligation for dsDNA,[44] small DNA nanostructure,[45] and DNA origami.[24] For instance, the native ligation by EDC on a small DNA nanostructure with 5–6 scaffold nicks (staples were not ligated, 3–4 days reaction) resulted in the ligation yield of ≈7% of the target product of 600 bases in length along with several short strands.[45] The same with T4 DNA ligase (24 h reaction) and CNBr (1-60 min reaction) failed to yield the full-length product, while resulted in the strands with only 300 and 400 bases, respectively, of unspecified reaction yields. We have achieved near quantitative yields of the native ligation of the full-size DNA origami containing 226 nicks within 5 min, emphasizing the significant advantages of the current methods over a few available reports.[24] Also, we anticipate that these ligation methods can be successfully applied to other origami designs. It is worth mentioning that these methods complement each other, and the choice depends on the requirements. CNBr-method may not be suitable for sensitive cases due to the HBr liberation. DMSO-method is mild and can be applied for sensitive cases, while it works only for 2D origami.

4. Conclusion

In summary, we have demonstrated two methods and optimized their conditions to ligate the staple nicks in 2D and 3D DNA origami with near quantitative ligation yields. These methods were successfully tested on eight different origami structures. DMSO enhances the reaction rate of the enzymatic reaction, reduces the amount of enzyme needed, and enhances ligation efficiency. In this case, though a 1 h reaction resulted in a significant ligation efficiency, an overnight reaction is needed for the reaction to saturate. Both methods lead to successful ligation of 2D origami, whereas chemical ligation is the only choice for 3D origami, indicating that the enzyme accessibility problem cannot be solved on 3D structure even by DMSO. The advantages of CNBr-mediate ligation are the faster reaction time of 5 min, quantitative reaction yield, and native phosphate ligation. Finally, the ligation of origami enhances its stability against thermal treatments, during electrophoresis and purification, against nuclease, and cell lysate. Proof-of-concept experiments on DNA origami for its use in drug and vaccine deliveries and virus inhibition have emerged, while its stability issues remain ever elusive. We anticipate that this study will be a stepping stone toward realizing such a real-life application of stable origami.

5. Experimental Section

Phosphorylation of Staple Strands: Before the phosphorylation reaction, all the staples were purified and buffer exchanged into Tris-HCl (10 mM, pH 7.5) containing NaCl (20 mM) by using Micro Bio-Spin P-6 columns to get rid of any kinase inhibitors. The staple oligoDNAs were then phosphorylated at the 5′-end using PNK. In a typical reaction, the staples (160-280 nM of individual strand concentration) and ATP mixture (staples:ATP = 1:2) were taken in 1× PNK buffer (50 mM of Tris-HCl, pH 7.5, 10 mM of $MgCl_2$, and 5 mM of dithiothreitol). PNK (20 U) was added to the reaction mixture and incubated at 37 °C for 30 min. After the reaction, PNK was heat denatured at 70 °C for 10 min. Since the PNK buffer is compatible with all 2D origami folding, the staples after the PNK reaction were used without purification. However, the 3D origami staples were exchanged into the desired folding buffers (wide infra). Phosphorylation of the staples is necessary irrespective of the method of ligation used in this study. All enzyme concentrations in the unit (U) are related to the reaction volume of 50 µL.

DNA Origami Folding: After the staple phosphorylation, M13mp18 (40 nM) was added to the reaction mixtures and thermally annealed. The M13 DNAs used contained 7249 bases (all 2D origami, HPO, and HPC), 7308 bases (SPH), and 8064 bases (Ring). The following annealing conditions were used to fold the origami: i) all 2D origami: 95-4 °C: incubated at 95 °C for 1 min, rapidly cooled down to 53 °C and incubated for 30 min, then rapidly cooled down to 4 °C; ii) HPO and HPC: 90-10 °C: incubated at 90 °C for 1 min, rapidly cooled down to 80 °C, cooled down to 60 °C at a rate of −1 °C per 5 min, and finally cooled down to 10 °C at a rate of −1 °C per 75 min; iii) SPH: 80–4 °C: incubated at 80 °C for 5 min, cooled down to 65 °C at a rate of −1 °C per 5 min and incubated for 20 min, slowly cooled down to 25°C at a rate of −1 °C per 20 min and incubated for 20 min, and rapidly cooled down to 4 °C; and iv) Ring: 80-15 °C: incubated at 80 °C for 5 min, cooled down to 65 °C at a rate of −1 °C per 5 min and incubated for 20 min, slowly cooled down to 25 °C at a rate of −1 °C per 50 min, and rapidly cooled down to 15 °C. The M13:staple ratios were 1:4 (all 2D origami and SPH), 1:5 (HPO and HPC), and 1:6 (Ring). The 3D origami was folded in a buffer containing 5 mM of Tris-base, pH 8, and 1 mM of EDTA with varying amounts of $MgCl_2$ (8, 12, and 14 mM for HPO and HPC, Ring, and SPH, respectively).

DMSO-Assisted Enzymatic Ligation: After the origami folding, the solutions were purified to remove the excess staples and PNK, and buffer exchanged into Tris-HCl (10 mM, pH 7.5) containing NaCl (20 mM) for 2D origami and 1× origami buffer (40 mM of Tris-base, pH 8.2, 20 mM of acetic acid, and 12.5 mM of $MgCl_2$) for 3D origami by using sephacryl S-300 gel filtration column. The absorptions of the purified origami were then measured by NanoDrop-2000 spectrophotometer (ThermoFisher Scientific), and the concentrations were calculated using the estimated molar absorption coefficient of the origami ($\epsilon_{260\,nm} = 12.4 \times 10^7\ M^{-1}\ cm^{-1}$).[23] From the known concentration of the purified samples, 15 nM of origami was taken in 1× PNK buffer that contained 0.5 mM ATP and the cosolvent (0 to 32%, v/v, as indicated). The cosolvents used were DMSO, methanol, ethanol, 2-propanol, acetone, dioxane, DMF, acetonitrile, and 2,2,2-trifluoroethanol (TFE), and the cosolute PEG 6000 was also used. After the initial experiment, only DMSO was used as a cosolvent as it performed the best. Then, T4 DNA ligase (0 to 4800 U, as indicated) was added to the reaction mixtures and incubated overnight (or as mentioned) at the indicated temperatures (4 °C, 16 °C, RT, 37 °C, 42 °C, and 47 °C). For comparison, the non-ligated and ligated samples without cosolvent were also prepared and treated under similar conditions. After the ligation reaction, 40 nM of the non-phosphorylated staples were added to the reaction mixtures that are necessary for better recovery of origami during the second purification, and purified and buffer exchanged into 1× origami buffer by using the gel filteration column. The purified samples were quantified by using NanoDrop and used for further analyses. Note that unless otherwise mentioned, the cosolvents and cosolute concentrations are presented in v/v and w/v, respectively.

Chemical Ligation by CNBr: For the chemical ligation of origami, the CNBr-based method previously reported for the duplex DNAs by Shabarova et al. was adapted.[26,44] The conditions for the phosphorylation, origami folding, gel filteration column purifications, and quantification by NanoDrop are the same as above, except that MES buffer (1 M, pH 7.6) was used for the buffer exchanging process. From the purified origami, 15 nM of each sample in MES buffer was taken and kept the mixtures on the ice. The ice-cold CNBr solution in acetonitrile (0.5 M) was added to the reaction mixtures, gently vortexed, and incubated on the ice at the indicated time (5-20 min). After the reaction, the samples were immediately purified and exchanged into 1× origami buffer using Micro Bio-Spin P-6 column (only for PAGE) or S-300, quantified, and used for further analyses.

Native AGE Analysis: Typically, each origami sample (3 nM) was mixed with orange G loading dye (1×) and loaded into a 1% agarose gel. The gels were run using 1× TBE running buffer at 100 V and 4 °C. The gel and running buffer contained 5 mM of $MgCl_2$ or NaCl only for the mentioned cases. After the electrophoresis, the gels were stained using ethidium bromide (EtBr) in 1× TBE for 30 min, and the images were recorded on a ChemiDoc Imaging Systems (Bio-Rad). The relative retention factor (R_f) of each band in the AGE was calculated in reference to the migration of the non-ligated native origami from the sample loading well using the following equation:

$$R_f = \left(L_{Ligated} - L_{Native}\right) / L_{Native} \quad (1)$$

where $L_{Ligated}$ and L_{Native} are the migration lengths of the ligated and native origami bands, respectively, from the sample loading wells.

To extract the DNA origami, AGE was performed as described above. The target band was identified by excising a portion of the gel, staining it with EtBr, and capturing an image. The target band was then excised and samples were extracted using the freeze and squeeze DNA gel extraction spin column (Bio-Rad).

Denaturing PAGE: Since the origami precipitation was observed at higher amounts of DMSO (see Results Section), the spin column filtration after the ligation reaction was omitted for the PAGE analyses. Instead, the samples were freeze-dried on a lyophilizer (Asahi Life Science) to concentrate them to allow the addition of 80–90% (v/v) of formamide for the denaturing analyses. After adding formamide, the samples were denatured at 95 °C for 10 min and rapidly cooled down on the ice. The denatured samples were then loaded into a 12% PAGE containing 8 M urea. Low molecular weight DNA ladder (NEB, England) was also denatured similarly but without lyophilization and loaded into the gel. The gels were run using 1× TBE buffer at 300 V and RT. The gels were then stained using EtBr in 1× TBE for 20 min and then imaged. The ligation efficiencies were calculated by subtracting the unligated band intensities from the total band intensities. The correction factor for excess unpurified staples (≈10%) was also added to the yield values. Due to the complex nature of the staple designs and the large number of staples, it was difficult to estimate the actual number of nicks ligated. While the reported ligation efficiencies indicate the percentage of the strands that were ligated at least once.

UV-Melting Analysis: The melting patterns of the non-ligated and ligated origami were analyzed by using a UV-visible spectrophotometer (UV-2600i, Shimadzu) equipped with a Peltier system for temperature control. Typically, the purified samples (each 100 µL of 4 nM) in 1× origami buffer were taken in the 8 series micro multi-cell (10 mm path length). The melting was carried out from 25–95 °C with a heating rate of 0.5 °C min^{-1}, and the absorbance at 260 nm of each sample was recorded at every 0.5 °C. The 1× origami buffer was used for blank correction. The T_m values were derived from the peak observed in the derivative plots. The hypochromicity values were calculated using the following equation:

$$\text{hypochromicity}\ (\%) = \left[\left(A_{Native} - A_{Ligated}\right) / A_{Native}\right] \times 100 \quad (2)$$

where A_{Native} and $A_{Ligated}$ are the absorbances of the native and ligated origami at 260 nm, respectively.

AFM Imaging: AFM images were recorded under the tapping mode using a Sample Scanning-Nano Explorer AFM system (SS-NEX, RIBM, Tsukuba) with a silicon nitride cantilever (resonant frequency: 1.5 MHz,

spring constant: 0.1 N m^{-1}, Olympus).[46] For the stability analyses, the purified samples were incubated discretely at the indicated temperature for 10 min, rapidly cooled down on the ice, and kept on ice until imaging. The sample (2 µL of 1–2 nM) was incubated on a freshly cleaved mica surface (ϕ 1.5 mm) for 5 min at RT. The surface was gently washed using 1× origami buffer, and images were recorded in the same buffer. For the estimation of the fraction of stable structures, at least 100 origami were counted from the AFM images.

Stability Analysis of Origami Against DNase I: The purified native or ligated origami (5 nM) was mixed with a known concentration (0.05 U only for AFM) of DNase I in 1× DNase I reaction buffer. The reaction mixtures were incubated at 37 °C for 1 h. The samples were then directly loaded into AGE or purified and buffer exchanged into 1× origami buffer for AFM analysis. The digestion yields were estimated by counting the fully intact origami structures as well as the partially digested origami observed in the AFM images.

Cell Culture: HEK293 cells (ATCC) were cultured in Dulbecco's modified eagle's medium (DMEM, Gibco) supplemented with 10% fetal bovine serum (FBS), 30 U mL^{-1} penicillin, and 30 µg mL^{-1} streptomycin at 37 °C under 5% CO_2 with 100% humidity.

Cell Lysis: The cells were washed with DMEM, collected in a centrifuge tube, and centrifuged for 5 min at 450 × g. The supernatant was discarded, repeated the same step, and the collected cell pellet was resuspended in CellLytic M reagent. The cells were incubated on a shaker for 15 min. The lysate was centrifuged at 15 000 × g for 15 min to pellet the cellular debris. The protein-containing supernatant was collected in a chilled test tube. The lysate was then diluted to the required concentration by lysis buffer (DMEM + PBS).

Stability Analysis of Origami with Cell Lysate: The native or ligated origami (5 nM) was mixed with the known concentration (10 000 cells only for AFM) of cell lysate and incubated for 12 h at RT. After the reaction, the samples were analyzed by AGE or AFM. Before AFM analysis, the samples were purified and buffer exchanged into 1× origami buffer and images were recorded in the same buffer. The scission yields were estimated by counting the structurally intact and scissioned origami structures observed in the AFM images.

Supporting Information

Supporting Information is available from the Wiley Online Library or from the author.

Acknowledgements

K.K. and A.R. contributed equally to this work. The authors thank the Ministry of Education, Culture, Sports, Science and Technology (MEXT, Japan) for the Grants-in-Aid for Scientific Research to A.R. (16K17934 and 21K05274), E.N. (20H02860 and 22H05418), and T.M. (17H01213 and 23H02083), and JST CREST to T.M. (JPMJCR18H5). A.R. thanks The Kyoto University Foundation for the research grant. A.R. and E.N. thank the Institute of Advanced Energy, Kyoto University, for the Research Grant for the Collaboration Program of the Laboratory for Complex Energy Processes. K.K. thanks the MEXT-SGU for a scholarship.

Conflict of Interest

The authors declare no conflict of interest.

Data Availability Statement

The data that support the findings of this study are available in the supplementary material of this article.

Keywords

cell lysate, chemical ligation, cosolvents, DNA origami, nuclease

Received: August 4, 2023
Published online: September 21, 2023

[1] P. W. K. Rothemund, *Nature* **2006**, *440*, 297.
[2] A. Rajendran, M. Endo, Y. Katsuda, K. Hidaka, H. Sugiyama, *ACS Nano* **2011**, *5*, 665.
[3] a) X. Liu, F. Zhang, X. Jing, M. Pan, P. Liu, W. Li, B. Zhu, J. Li, H. Chen, L. Wang, J. Lin, Y. Liu, D. Zhao, H. Yan, C. Fan, *Nature* **2018**, *559*, 593; b) S. Ramakrishnan, S. Subramaniam, A. F. Stewart, G. Grundmeier, A. Keller, *ACS Appl. Mater. Interfaces* **2016**, *8*, 31239.
[4] a) A. Rajendran, M. Endo, H. Sugiyama, *Angew. Chem., Int. Ed.* **2012**, *51*, 874; b) A. Rajendran, E. Nakata, S. Nakano, T. Morii, *ChemBioChem* **2017**, *18*, 696.
[5] V. Linko, A. Ora, M. A. Kostiainen, *Trends Biotechnol.* **2015**, *33*, 586.
[6] A. Rajendran, M. Endo, Y. Katsuda, K. Hidaka, H. Sugiyama, *J. Am. Chem. Soc.* **2011**, *133*, 14488.
[7] M. Hanke, E. Tomm, G. Grundmeier, A. Keller, *ChemBioChem* **2023**, *24*, 202300338.
[8] M. Endo, K. Hidaka, H. Sugiyama, *Org. Biomol. Chem.* **2011**, *9*, 2075.
[9] a) D. Wang, Z. Da, B. Zhang, M. A. Isbell, Y. Dong, X. Zhou, H. Liu, J. Y. Y. Heng, Z. Yang, *RSC Adv.* **2015**, *5*, 58734; b) N. Wu, I. Willner, *Nano Lett.* **2016**, *16*, 6650; c) E. Nakata, H. Hirose, K. Gerelbaatar, J. V. V. Arafiles, Z. Zhang, S. Futaki, T. Morii, *Chem. Sci.* **2021**, *12*, 8231.
[10] C. Kielar, Y. Xin, B. Shen, M. A. Kostiainen, G. Grundmeier, V. Linko, A. Keller, *Angew. Chem., Int. Ed.* **2018**, *57*, 9470.
[11] C. E. Castro, F. Kilchherr, D.-N. Kim, E. L. Shiao, T. Wauer, P. Wortmann, M. Bathe, H. Dietz, *Nat. Methods* **2011**, *8*, 221.
[12] J. Hahn, S. F. J. Wickham, W. M. Shih, S. D. Perrault, *ACS Nano* **2014**, *8*, 8765.
[13] H. Bila, E. E. Kurisinkal, M. M. C. Bastings, *Biomater. Sci.* **2019**, *7*, 532.
[14] V. Linko, A. Keller, *Small* **2023**, *19*, 2301935.
[15] V. Linko, B. Shen, K. Tapio, J. J. Toppari, M. A. Kostiainen, S. Tuukkanen, *Sci. Rep.* **2015**, *5*, 15634.
[16] S. Ramakrishnan, H. Ijäs, V. Linko, A. Keller, *Comput. Struct. Biotechnol. J.* **2018**, *16*, 342.
[17] T. Gerling, M. Kube, B. Kick, H. Dietz, *Sci. Adv.* **2018**, *4*, eaau1157.
[18] S. D. Perrault, W. M. Shih, *ACS Nano* **2014**, *8*, 5132.
[19] J. Mikkilä, A.-P. Eskelinen, E. H. Niemelä, V. Linko, M. J. Frilander, P. Törmä, M. A. Kostiainen, *Nano Lett.* **2014**, *14*, 2196.
[20] A. Hernandez-Garcia, N. A. Estrich, M. W. T. Werten, J. R. C. Van Der Maarel, T. H. Labean, F. A. De Wolf, M. A. Cohen Stuart, R. De Vries, *ACS Nano* **2017**, *11*, 144.
[21] N. P. Agarwal, M. Matthies, F. N. Gür, K. Osada, T. L. Schmidt, *Angew. Chem., Int. Ed.* **2017**, *56*, 5460.
[22] A. Chopra, S. Krishnan, F. C. Simmel, *Nano Lett.* **2016**, *16*, 6683.
[23] A. Rajendran, K. Krishnamurthy, A. Giridasappa, E. Nakata, T. Morii, *Nucleic Acids Res.* **2021**, *49*, 7884.
[24] N. Weizenmann, G. Scheidgen-Kleyboldt, J. Ye, C. B. Krause, D. Kauert, S. Helmi, C. Rouillon, R. Seidel, *Nanoscale* **2021**, *13*, 17556.
[25] K. Murayama, H. Okita, T. Kuriki, H. Asanuma, *Nat. Commun.* **2021**, *12*, 804.
[26] a) O. A. Fedorova, M. B. Gottikh, T. S. Oretskaya, Z. A. Shabarova, *Nucleosides and Nucleotides* **1996**, *15*, 1137; b) Z. A. Shabarova, I. N. Merenkova, T. S. Oretskaya, N. I. Sokolova, E. A. Skripkin, E. V. Alexeyeva, A. G. Balakin, A. A. Bogdanov, *Nucleic Acids Res.* **1991**, *19*, 4247.
[27] T. E. England, O. C. Uhlenbeck, *Nature* **1978**, *275*, 560.

[28] R. C. Alexander, *Nucleic Acids Res.* **2003**, *31*, 3208.
[29] Z.-X. Xiao, H.-M. Cao, X.-H. Luan, J.-L. Zhao, D.-Z. Wei, J.-H. Xiao, *Mol. Biotechnol.* **2007**, *35*, 129.
[30] M. Endo, Y. Katsuda, K. Hidaka, H. Sugiyama, *J. Am. Chem. Soc.* **2010**, *132*, 1592.
[31] T. A. Ngo, E. Nakata, M. Saimura, T. Morii, *J. Am. Chem. Soc.* **2016**, *138*, 3012.
[32] E. Nakata, F. F. Liew, C. Uwatoko, S. Kiyonaka, Y. Mori, Y. Katsuda, M. Endo, H. Sugiyama, T. Morii, *Angew. Chem., Int. Ed.* **2012**, *51*, 2421.
[33] a) S. M. Douglas, I. Bachelet, G. M. Church, *Science* **2012**, *335*, 831; b) P. Lin, H. Dinh, E. Nakata, T. Morii, *Chem. Commun.* **2021**, *57*, 11197.
[34] Y. Yang, J. Wang, H. Shigematsu, W. Xu, W. M. Shih, J. E. Rothman, C. Lin, *Nat. Chem.* **2016**, *8*, 476.
[35] S. Ramakrishnan, B. Shen, M. A. Kostiainen, G. Grundmeier, A. Keller, V. Linko, *ChemBioChem* **2019**, *20*, 2818.
[36] S.-I. Nakano, N. Sugimoto, *Biophys. Rev.* **2016**, *8*, 11.
[37] a) S. Roy, B. Jana, B. Bagchi, *J. Chem. Phys.* **2012**, *136*, 115103; b) D. H. Pliura, J. B. Jones, *Can. J. Chem.* **1980**, *58*, 2633.
[38] A. K. Behera, K. J. Schlund, A. J. Mason, K. O. Alila, M. Han, R. L. Grout, D. A. Baum, *Biopolymers* **2013**, *99*, 382.
[39] S. Cui, J. Yu, F. Kühner, K. Schulten, H. E. Gaub, *J. Am. Chem. Soc.* **2007**, *129*, 14710.
[40] M. A. Jensen, M. Fukushima, R. W. Davis, *PLoS One* **2010**, *5*, e11024.
[41] P. R. Winship, *Nucleic Acids Res.* **1989**, *17*, 1266.
[42] T. Zhang, C. Shang, R. Duan, A. Hakeem, Z. Zhang, X. Lou, F. Xia, *Analyst* **2015**, *140*, 2023.
[43] K. Shi, T. E. Bohl, J. Park, A. Zasada, S. Malik, S. Banerjee, V. Tran, N. Li, Z. Yin, F. Kurniawan, K. Orellana, H. Aihara, *Nucleic Acids Res.* **2018**, *46*, 10474.
[44] Z. A. Shabarova, *Biochimie* **1988**, *70*, 1323.
[45] M. Kramer, C. Richert, *Chem. Biodivers.* **2017**, *14*, e1700315.
[46] A. Rajendran, M. Endo, H. Sugiyama, *Chem. Rev.* **2014**, *114*, 1493.

